Supporting Information

A New Universal Aqueous Conductive Binder *via* Esterification Reinforced Electrostatic/H-bonded Self-assembly for High Areal Capacity and Stable Lithium-Ion Batteries

Farong Zhang[a#], Hongyu Xia[a#], Tongye Wei[b]*, Huaming Li[a,c], Mei Yang[a,c]*, An-Min Cao[d]*

[a] College of Chemistry, Xiangtan University, Xiangtan 411105, Hunan Province, P. R. China

[b] Hunan Institute of Advanced Sensing and Information Technology, Xiangtan University, Xiangtan 411105, Hunan Province, P. R. China

[c] Key Laboratory of Polymeric Materials & Application Technology of Hunan Province, Key Laboratory of Advanced Functional Polymeric Materials of College of Hunan Province, and Key Lab of Environment-Friendly Chemistry and Application in Ministry of Education, Xiangtan University, Xiangtan 411105, Hunan Province, P. R. China

[d] CAS Key Laboratory of Molecular Nanostructure and Nanotechnology and Beijing National Laboratory for Molecular Sciences, Institute of Chemistry, Chinese Academy of Sciences (CAS), Beijing 100190, P. R. China; University of Chinese Academy of Sciences, Beijing 100049, P. R. China

*Corresponding author. E-mail address: yangmei@xtu (M. Yang) weity@xtu.edu.cn (T. Wei) anmin_cao@iccas.ac.cn (A-M. Cao)

Experimental Section

Materials. PAA (Mw = 460000), 6-amino-1-hexanol (AH), ethyl alcohol were purchased from shanghai Aladdin biochemical technology Co., Ltd. Hidrosoluble carboxylic WMCNT was purchased from Jiangsu Cnano Technology Co., Ltd, composing MWCNT (d =7~11 nm) of 4±0.15 wt%, and dispersant of 1.25±0.05 wt%. Silicon carbon composite material was purchased from Anhui Keda New Material Co., Ltd and its theoretical specific capacity is ~550 mAh g^{-1}.

Characterization. Fourier transform infrared (FTIR) spectra were recorded on Nicolet 650 spectrophotometer. Scanning electron microscopy (SEM) imaging was performed on S-4800 (JEOL) at an acceleration voltage of 10 kV. Powder X-ray diffraction (XRD) was conducted on a Rigaku D/Max 2500PC diffractometer. Thermal gravimetric analysis (TGA) was carried out on SDT Q600 with a heating rate of 5 ^{o}C min^{-1} under O_2 or N_2 protection.

Contact Angle test procedure: (1) Place the sample on the contact angle test platform and then turn on the test light source and test software. Make sure the sample is under the level condition; (2) Fill the pipette with the liquid to be measured, then set the droplet volume and push the droplet out to hang on the pipette tip; (3) Push the pipette slowly downward until the droplet makes contact with the sample surface, then immediately return the pipette to its position; (4) When it is observed that the droplet is about to contact the sample, click the video recording button on the test software immediately to record the wetting process of the droplet on the sample surface in real time and capture images; (5) Output results.

Electrochemistry. The electrochemical performance were evaluated by using the CR2032-type

half cells, which were assembled by sandwiching a separator (polyolefin porous film) between the APA/CNTbased or PAA-based working electrode and Li foil counter electrode. The active material loading of the APA/CNT based electrode was in the range of 1 to 15 mg cm^{-2}. The electrolyte was 1.0 M LiPF6 in a mixture of diethylene carbonate (DEC) and ethylene carbonate (EC) (1:1, v/v). The cycling and rate performances were carried out on NEWARE CT-4008 testing system. The electrochemical impedance spectra (EIS) and CV testing were all performed on the CHI760e electrochemical workstation. In the equivalent circuit diagram, Rb represents the resistance of bulk materials，its effect can be observed in Zreal (intersection of the x-axis and the plot). W_1 impedance affected by the lithium-ion diffusion process of the anode, which can be observed in the slope of the straight line after followed the arc. Besides, R_{SEI} originates from the impedance of the layer between the electrode and electrolyte, which produced by decomposition of the electrolyte. Rct associates with the kinetics of an electrochemical reaction caused by the particle size, surface coating, band gap structure and phase transition.[13]

DFT calculations. The Molecular structure optimization was performed by Guassian.[14] Different hydrogen bond configurations in PAA and APA were simulated by means of terminal sealing hydrogen.[15] Gauss's quantitative calculations were based on the idea that molecular orbitals are linear combinations of atomic orbitals.[16] The hydrogen bond strength and electron density are estimated simply and reliably by using the method of DFT calculation.

Supplementary Figures and Tables

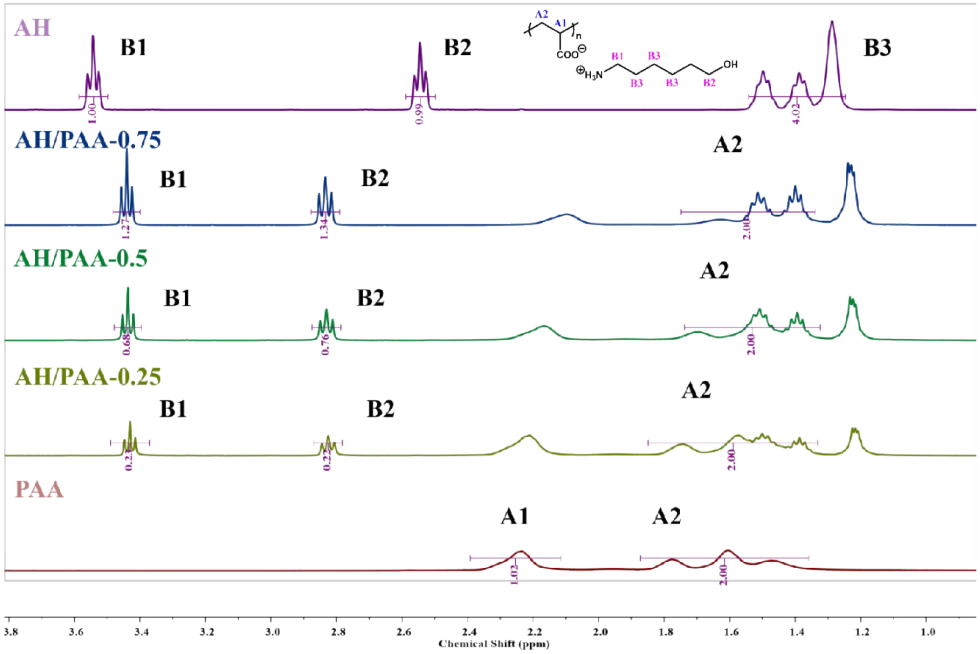

Fig. S1. ^{1}H NMR spectra of APA/CNT binders with variable AH/PAA ratio.

Table S1. The degree (x) of deprotonation of -COOH for APA binders with variable AH/PAA ratio.

Sample	Integral area (B1)	Integral area (A2)	x (%)
AH/PAA-0.25	0.23	2	11.5%
AH/PAA-0.50	0.68	2	34.0%
AH/PAA-0.75	1.27	2	63.5%

Since atom number is proportional to the integral peak area, the degree of deprotonation of the carboxyl group (x) can be calculated, according to follow equation:

$$x = \text{Integral area}_{B1} / \text{Integral area}_{A2}$$

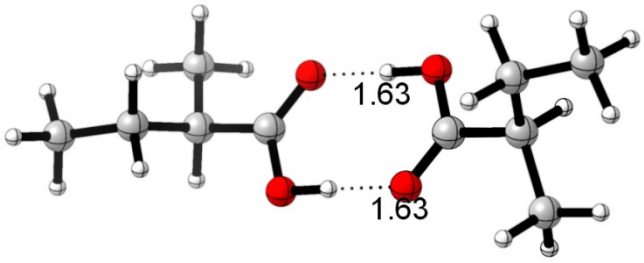

Fig. S2. H-bonds in APA by DFT caculation.

Table S2. The bond energy and electrons density of different hydrogen bonds.

Type	E (Kcal/mol)	Electrons density (a.u.)
–NH_3^+···HO–	-23.77	0.0683
–C=O···HO–	-19.40	0.0552
–COOH···HOOC–	-11.16	0.0511
–OH···OH–	-5.93	0.0286

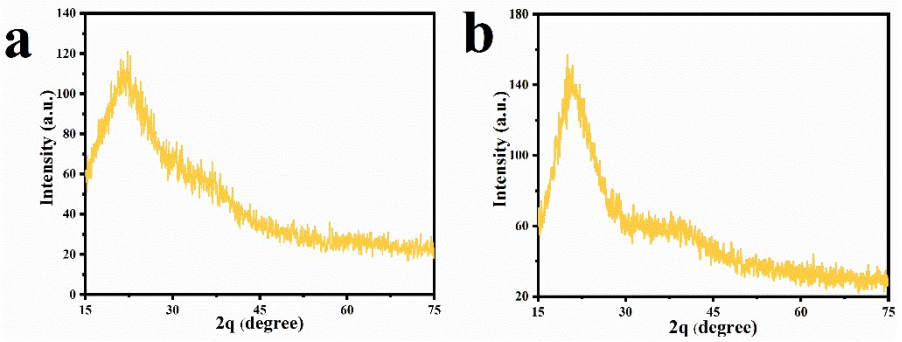

Fig. S3. X-ray diffraction (XRD) of (a) PAA and (b) APA/CNT.

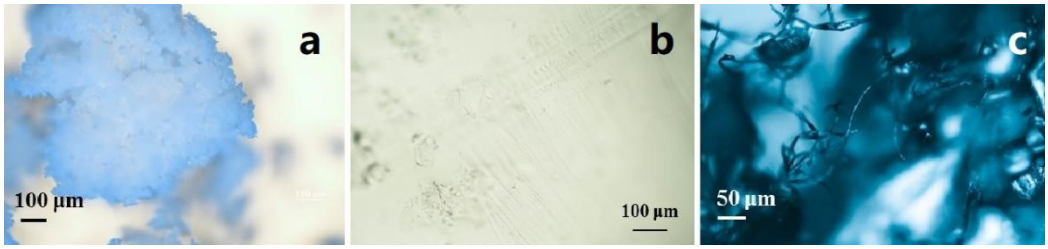

Fig. S4. The optical microscopy images of PAA (a), APA (b) and APA/CNT (e).

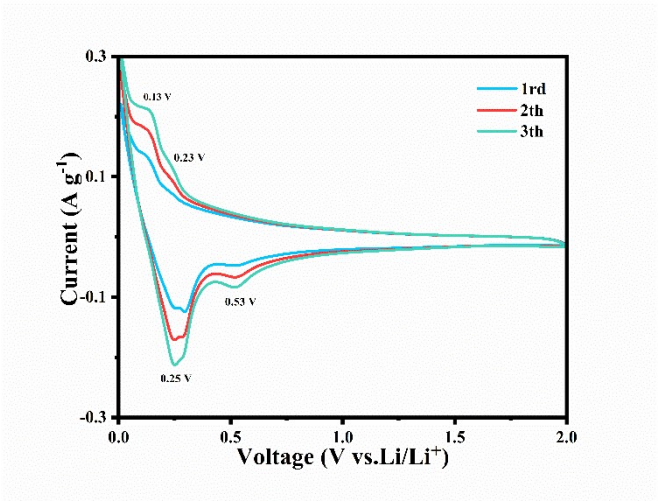

Fig. S5. CV curves of APA/CNT based electrode at 0.5 mV.

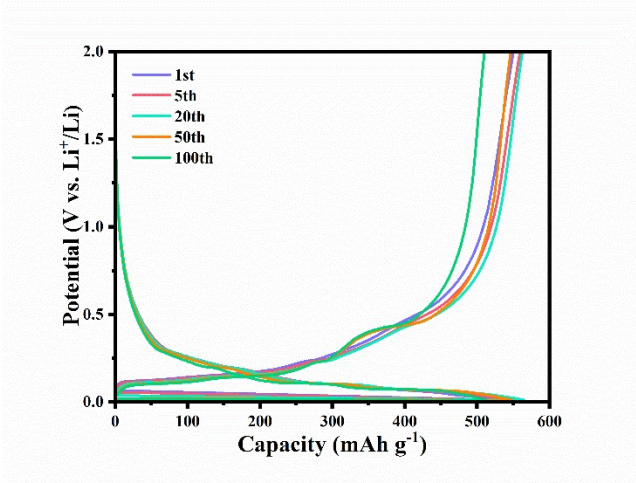

Fig. S6. The charge-discharge curves of APA/CNT based electrode at 0.2 A g^{-1}.

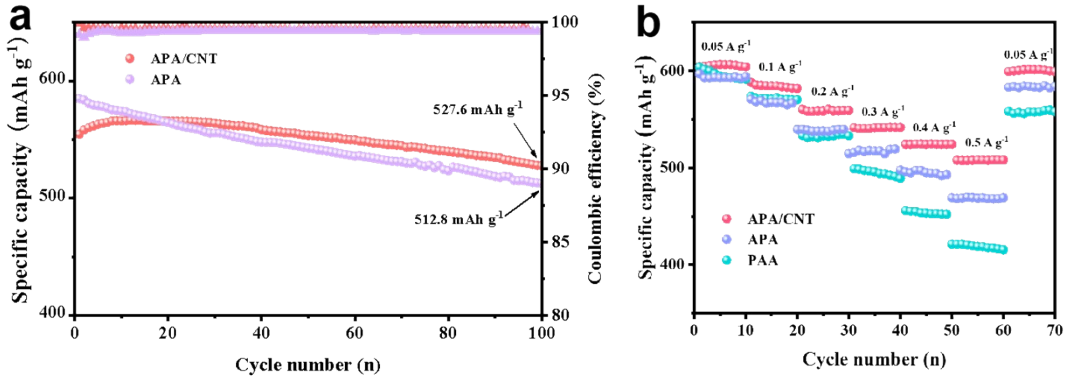

Fig. S7. The cycling (a) and rate (b) performance of PAA, APA and APA/CNT based Si/C anodes at 0.2 A g^{-1}.

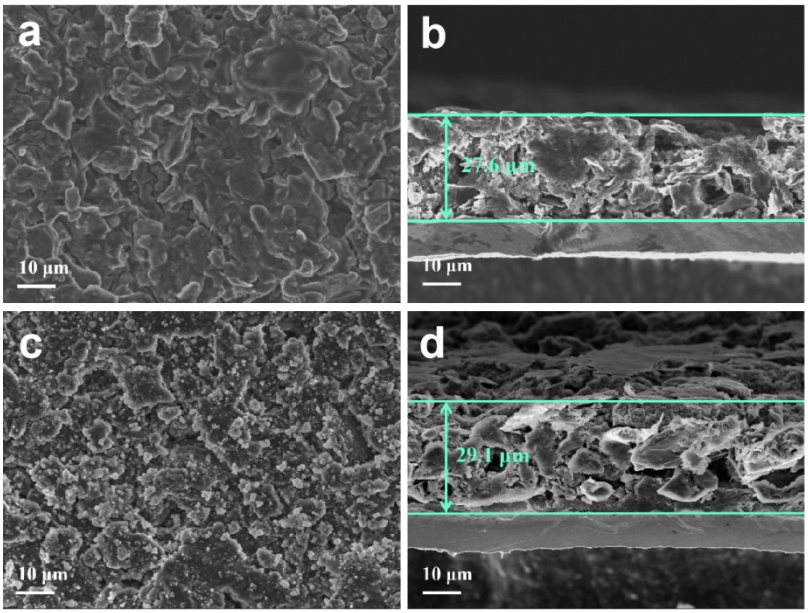

Fig. S8. The top-view and cross-sectional view of APA based Si/C anode before (a, b) and after (c, d) 100 cycles.

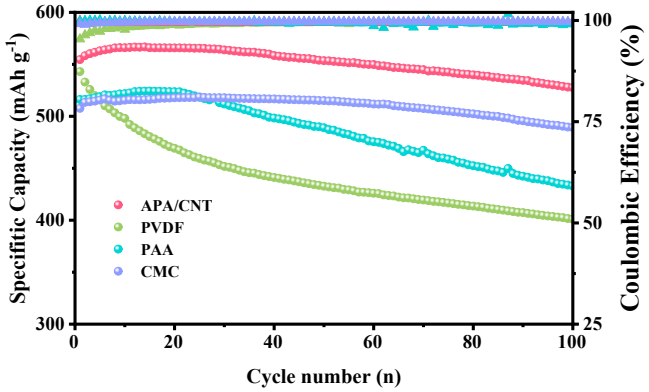

Fig. S9. The cycling performance of CMC, PVDF, PAA and APA/CNT based Si/C anodes.

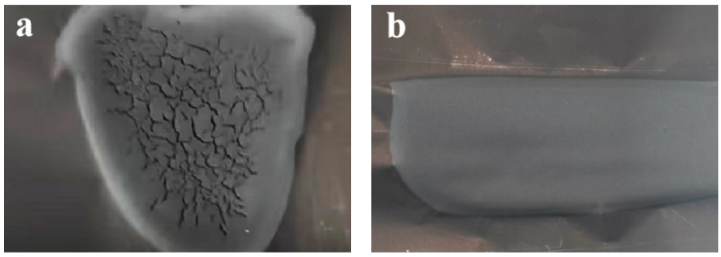

Fig. S10. Optical pictures of PAA and APA/CNT based thick (high-loaded) electrodes.

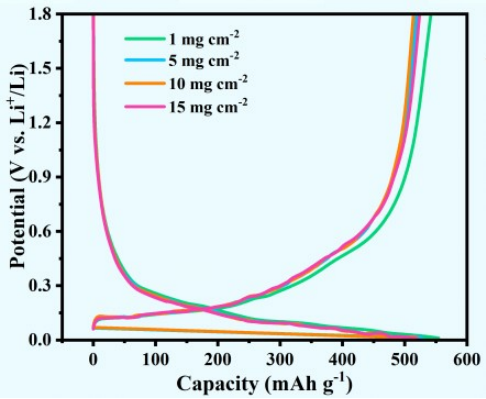

Fig. S11. Charge/discharge curves of the APA/CNT electrodes at different mass loadings.

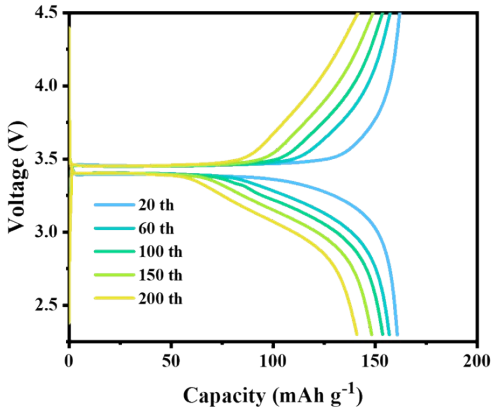

Fig. S12. Charge/discharge voltage profiles of APA/CNT based $LiFePO_4$ cathode.

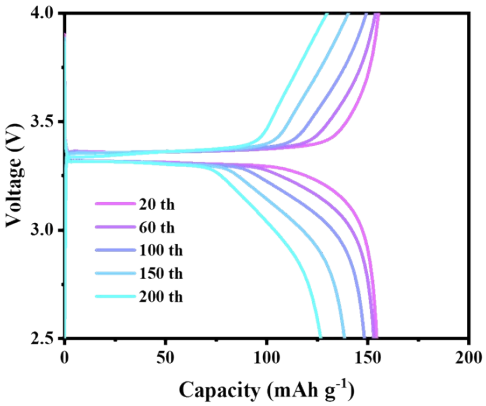

Fig. S13. Charge/discharge voltage profiles of APA/CNT based $LiFePO_4$/Si/C full cell.

References

[S1] L. Hu, M. Jin, Z. Zhang, H. Chen, F. Boorboor Ajdari, J. Song, *Adv. Funct. Mater.*, 2022, **32**, 2111560.

[S2] L. Hu, X. Zhang, P. Zhao, H. Fan, Z. Zhang, J. Deng, G. Ungar, J. Song, *Adv. Mater*., 2021, **33**, 2104416.

[S3] R. Kasinathan, M. Marinaro, P. Axmann, M. Wohlfahrt-Mehrens, *Energy Technol*., 2018, **6**, 2256.

[S4] B. Gendensuren, N. Sugartseren, M. Kim, E. Oh, *Chem. Eng. J*., 2022, **433**, 133553.

[S5]J. Kim, J. Choi, K. Park, S. Kim, K. W. Nam, K. Char, J. W. Choi, *Adv. Energy Mater*., 2022, **12**, 2103718.

[S6] L. Li, T. Li, Y. Sha, C. Zhang, B. Ren, L. Zhang, S. Zhang, *Ind. Eng. Chem. Res*. , 2021, **60**, 17399.

[S7] J. Kim, K. Park, Y. Cho, H. Shin, S. Kim, K. Char, J. W. Choi, *Adv. Sci*., 2021, **8**, 2004290.

[S8] P. Cao, M. Naguib, Z. Du, E. Stacy, B. Li, T. Hong, K. Xing, D. N. Voylov, J. Li, D. L. Wood, A. P. Sokolov, J. Nanda, T. Saito, *ACS Appl. Mater. Interfaces*, 2018, **10**, 3470.

[S9] S. Huang, J. Ren, R. Liu, Y. Bai, X. Li, Y. Huang, M. Yue, X. He, G. Yuan, *New J Chem*, 2018, **42**, 6742.

[S10] X. Li, H. Chen, M. Chen, J. Qi, S. Chen, H. Zhuo, *ACS Appl. Energy Mater*., 2021, **4**, 12709.

[S11] B. Gendensuren, E. Oh, *J. Power Sources*, 2018, **384**, 379.

[S12] L. Yu, Z. Luo, C. Gong, Y. Zheng, Z. Zhou, H. Zhao, Y. Xu, *Polym. J.*, 2021, **53**, 923.

[S13]Y. Su, X. Feng, R. Zheng, Y. Lv, Z. Wang, Y. Zhao, L. Shi, S. Yuan, *ACS Nano*., 2021, **15**, 14570.

[S14] G. Graziano, *Nat. Rev. Chem*., 2017, **1**, 0019.

[S15] S. Luber, *J. Chem. Theory Comput*., 2017, **13**, 1254.

[S16] Y. Mei, J. Yu, Z. Chen, N. Q. Su, W. Yang, *J. Chem. Theory Comput*., 2022, **18**, 840.